PNAS
www.pnas.org

Supplementary Information for

Transgenerational hypocortisolism and behavioral disruption are induced by the antidepressant fluoxetine in male zebrafish *Danio rerio*

Marilyn N. Vera-Chang[a,b], Antony D. St-Jacques[c,d], Rémi Gagné[e], Chris J. Martyniuk[f,g,h], Carole L. Yauk[e], Thomas W. Moon[a,b], and Vance L. Trudeau[a,b,1]

[a] Department of Biology, University of Ottawa, Ottawa, ON K1N 6N5, Canada
[b] Centre for Advanced Research in Environmental Genomics, University of Ottawa, Ottawa, ON K1N 6N5, Canada
[c] Department of Chemistry and Biomolecular Sciences, University of Ottawa, Ottawa, ON K1N 6N5, Canada
[d] Centre for Catalysis Research and Innovation, University of Ottawa, Ottawa, ON K1N 6N5, Canada
[e] Environmental Health Science and Research Bureau, Health Canada, Ottawa, ON K1A 0K9, Canada
[f] Center for Environmental and Human Toxicology, University of Florida, Gainesville, FL 32611
[g] Department of Physiological Sciences, University of Florida, Gainesville, FL 32611
[h] University of Florida Genetics Institute, University of Florida, Gainesville, FL 32611

[1] To whom correspondence should be addressed. Email: trudeauv@uottawa.ca

This PDF file includes:

Supplementary text
Figs. S1 to S6
Tables S1 to S9
References for SI reference citations

www.pnas.org/cgi/doi/10.1073/pnas.1811695115

Supplementary Information Text

SI Materials and methods

Transgenerational animals and in vivo exposures. All procedures conducted in this study were approved by the University of Ottawa Animal Care Protocol Review Committee and are in compliance with the guidelines of the Canadian Council on Animal Care for the use of animals in research. Adult ZF of the AB strain were obtained from Big Al's Aquarium in Ottawa, Ontario and allowed to acclimate for 4 weeks prior to generating the parents of the F_0 generation (F_{-1}). The sex ratio of the F_{-1} (~1F:1M) ensured our founder fish (F_0) originated from a balanced population without any genetic predisposition to a certain sex. The fish in the generation F_{-1} were subsequently bred to produce the F_0 which was used to generate the CTR and the two FLX-exposed lineages for the F_1 to F_3 generations (see Fig. S4).

To model human fetal exposures, one group of F_0 embryos was exposed to the nominal concentration of 54 $\mu g \cdot L^{-1}$ FLX (HFL), which is within the range detected in the cord blood of FLX-treated pregnant women (1-3). Stock solutions (4 $mg \cdot mL^{-1}$) were prepared by direct addition of 12.5 mL Milli-Q water to 50 mg Fluoxetine-HCL (Millipore Sigma Cat. # F132) and the concentration confirmed by the method of Joana and Zélia (4). Even though both FLX and its metabolite norFLX have been detected in the cord blood of FLX-treated pregnant women as well as in the plasma of newborns (2, 3, 5) and that norFLX is slightly more potent at blocking the 5-HT transporter (the main target of FLX and norFLX) (6), FLX was used in this study since it has been showed that the inhibition of the 5-HT transporter is only one of the mechanisms by which FLX exerts its therapeutic actions. The other mechanisms which involves the hippocampus and hypothalamus (7-9) have not been well studied with regards to the effects of norFLX. Therefore, due to the

diverse mechanistic actions of FLX, its exposure could contribute to a wider range of side effects. To model exposures of wild fish, another group of F_0 embryos was exposed to 0.54 $\mu g \cdot L^{-1}$ FLX (LFL), which is environmentally relevant to fish exposed to pharmaceutical pollutants released from sewage treatment plants (10). We have previously studied the short-term effects of both concentrations on the reproductive and metabolic physiology of adult goldfish *Carassius auratus* (10, 11) and ZF (12). Concentrations of FLX in exposure solutions prepared by serial dilution of stock were quantified against a standard curve (3 x 10^{-11} to 3 x 10^{-4} $mg \cdot ml^{-1}$; 4 µL injection volume) using the nano-LCMS/MS (Eksigent ekspert nanoLC 400, ThermoFisher Velose Pro) and found to be 77.5 ± 9.4 % of nominal expected concentrations, in general agreement with our previous studies (10).

All experimental fish in each generation were mated at 24 ± 2 weeks post-fertilization (wpf). Only virgin fish were used in this experiment to avoid potential confounding effects brought about by fish with different breeding experiences on their reproductive fitness. Fifteen breeding pairs were randomly chosen to generate founders (F_0) and all subsequent generations (F_1 – F_3). Pairs in F_0 to F_3 that did not spawn at trial 1 were provided a second opportunity with a different mate randomly chosen from non-spawning individuals within the same lineage to eliminate the possibility of mate preference, which has been extensively studied in ZF (13-15). Sex ratios, reproductive fitness, condition factor and developmental outcomes of the descendants were monitored throughout the study; however, no significant changes were observed.

Mating pairs were set up in the late afternoon in crossing cages (Aquatic Habitats) with a plastic divider that separated the female from the male and left undisturbed until the

following morning. The crossing cages were composed of a 1-L holding tank (crossing cage) and an additional container that was inserted inside the cage. The bottom of this inner-container was perforated with small holes which allowed eggs to fall down into the cage and be protected from predation. On the day of the spawning, the inner-container which held the fish was transferred to a new cage containing fresh system water. Extra care was taken to prevent any unnecessary stress of the fish during the transfer. The pairs were then allowed to spawn for 1 h, 45 min between 0900 and 1100 h. Eggs were immediately collected, submerged in 0.0075% bleach for 2 min, rinsed and counted. All fertilized eggs were kept, yielding a minimum population of 150 adult fish (at 20 wpf) per lineage in each generation. At 3 hpf, embryos were randomly assigned to Petri dishes containing either embryo medium alone (embryos in: F_{-1}; CTR F_0; and F_1 to F_3) or supplied with one of the two FLX (Millipore Sigma) concentrations (embryos in F_0 - FLX lineages). The exposure of the F_0 embryos (CTR and FLX lineages) was performed in glass Petri dishes from 3 hpf to 6 dpf during the critical period of ZF brain development (16). The F_1 to F_3 embryos from each lineage were distributed in plastic Petri dishes and labeled with the number assigned to their parents to monitor for any embryonic or larval developmental effect resulting from a specific mating pair. Embryos from all the generations were reared in Petri dishes until 6 dpf at a maximum density of 1 embryo·mL^{-1} and maintained at 28 °C without feeding to allow complete yolk sac absorption. Embryo medium was renewed daily and the appropriate concentrations of FLX replaced. Mortality and hatching were monitored daily during these 6 d and the surviving larvae from the same lineage were randomly distributed and transferred to a temperature-controlled ZF facility and reared in 1-L tanks containing heated (28.5 ± 0.2 °C), aerated, dechloraminated City of Ottawa tap water (system water)

at a density of 50 larvae·L^{-1} as per recommendation by Matthews, *et al.* (17). At this point, larvae were fed three times per day with Zebrafish Management Ltd. fry food diet of the appropriate size and according to their developmental stage and from 60 dpf until adulthood, fish were fed twice daily with No.1 crumble-Zeigler (Aquatic Habitats). The commercial feed in all stages from 16 dpf was supplemented with live *Artemia* nauplii (Artemia International LLC) once per day. The water was changed, and the debris was cleaned three times a week. At 30 dpf, juvenile fish were transferred into 3- and 10-L tanks (Aquatic Habitats) supplied with flow-through system water. To avoid high rearing density-induced masculinization and to reduce any effect on reproductive performance, adult fish were housed at a density of 5 fish·L^{-1} as suggested in the literature (17, 18). Larvae and adult ZF were maintained under a 14 h light:10 h dark photoperiod. In addition to temperature, water quality parameters including pH (7 – 7.5), conductivity (120 – 150 μS), ammonium nitrite and ammonium nitrate were checked periodically to ensure that they were within the appropriate range (19, 20). Fish from the same lineage in each generation were randomly mixed every month to avoid formation of social hierarchies and to reduce potential tank effects. All subsequent experimental testing described in this study was performed at 6 mpf. Therefore, at approximately 5 mpf, fish were separated by sex to minimize any handling stress during experiments and to prevent fish from spawning in the tanks.

Behavioral experiments and analyses. The novel-tank diving test adapted from Levin, *et al.* (21) was used to assess locomotor and exploratory activities of the fish evoked by their habituation response to novelty (22, 23). Adult females and males from each lineage in

generations F_0 to F_3 were placed in separate 3-L tanks (16 fish·tank^{-1}) and housed in the testing room one week prior to the experiment. The illumination, light cycle, temperature and water conditions of the testing room were similar to those of the main ZF facility. All behavioral testing in each generation was performed over a 3-day period, between 0930 and 1430 h on a stable surface with all environmental distractions kept to a minimum. At the end of the acclimatization period, each fish was individually placed in the trapezoid-shaped test tank (outside dimensions: 22.5 cm along the bottom × 28 cm at the top × 15 cm high × 7 cm width; Aquatic Habitats) filled with system water and their behavioral activity recorded from the front for 6 min in the absence of the camera operator. The test tank water was replaced with clean system water after each individual test. To enable a more efficient quantification of the ZF behavioral activities, the trapezoidal test tank underwent two different horizontal virtual divisions (Fig. S5), the first one was divided into two and the second into three equal zones. Videos were analyzed every 30 frames·s^{-1} for a total of 10,800 frames using an AT Python script. A Python script was also used to calculate the behavioral metrics (Table S1) assessed in this study. Briefly, the AT works by first converting the video file into still frames at a user defined frame per second rate, and subsequently segmenting the target object (fish) from the background in each frame of the video file. The segmentation procedure subtracts the background and identifies the fish by searching for an elliptical shape. The algorithm uses the position (coordinates) of the fish from the previous frames to eliminate moving objects with similar shapes including water droplets and feces. In case of possible conflicts with coordinates from the fish with other moving objects, the algorithm red-flags the specific frame and allows the user to manually select the target object. A ruler is included in the video recording for calibration. Tracking

began with the fish positioned at the bottom of the tank after the first 90 frames of the video by which the fish was allowed to recover from the stress of being released from the net and proceeded to the end of the video (10,800 frames). The script generates a video with the tracking patterns by displaying a dot on the tracked target to allow the user to verify that the tracked target is indeed the fish. Prior to the use of the AT algorithm on our experimental fish, the AT was validated to ensure reliable results. The Python scripts are available upon request.

Validation of the AT script. Thirty-one adult ZF fish of the AB strain, 16 females and 15 males, were used for the validation procedure of the AT algorithm. The 31 fish were subjected to the novel-tank diving test as previously described. The videos were then tracked using our developed AT algorithm and for comparison and data validation, the videos were also manually tracked using Logger Pro 3.13 (Vernier Software & Technology). Logger Pro is a data-collection and analysis software that allows for a frame by frame video analysis.

Tracking was conducted every 30 frames·s^{-1} beginning after the first 90 frames following the release of the fish from the net and with the fish positioned at the bottom of the tank and proceeded to the end of the video (10,800 frames; 6 min). The videos were first cropped using a Python script to ensure consistency of the video content for both tracking algorithms, the AT and the manual tracking (MT). Eighteen behavioral metrics were computed from the data (coordinates) acquired from the AT and MT (Table S8).

To validate the AT algorithm, the percent difference of each of the 18-behavioral metrics acquired from the AT and MT was calculated (Table S8). The percent difference

between both tracking systems ranged from 0.2 to 8.0%, with the highest variability observed in the maximum speed parameter. To reduce the dimensionality of the data and to further analyze these two datasets, PCA was performed using the 18-behavioral metrics obtained from the AT and MT. Female and male datasets were collectively analyzed for PC analysis. PC1 and PC2 strongly loaded most of the behavioral metrics and explained 56% and 23% of the behavioral variance, respectively (Table S9; Fig. S6*A*). Statistical analysis on PC1 and PC2 scores showed no significant difference between the datasets obtained from the AT and MT in neither females (Fig. S6*B*) nor males (Fig. S6*C*).

Transcriptomics. Whole-transcriptome sequencing (RNA-seq) was performed on adult male kidneys of the F_0 and F_3 generations that were individually collected, flash frozen on dry ice and stored at –80 °C. Total RNA was extracted using the RNeasy Plus Micro kit (Qiagen) and its integrity assessed using an Agilent Bioanalyzer 2100. The biological replicates sequenced in each lineage ranged from 5 to 8 individual males. Stranded mRNA libraries were built using the TruSeq Stranded mRNA Library Prep Kit for NeoPrep (Illumina) with 50 ng of total RNA. Libraries were pooled and sequenced on the NextSeq 500 with a 75 cycle flowcell, from which an average of 36 million reads per sample were obtained. Differential gene expression analyses were performed as follows: BCL files were converted for FASTQ files with BCL2FASTQ from Illumina and then CutAdapt (24) was used to trim adapters and polyGs tails. The STAR (25) aligner was used to map the reads on ZF (GRCz10 Ref 86) from Ensembl and the quality assessment/quality control of the libraries was evaluated with Qorts (26). Approximately 91.0% of the reads could be mapped to the genome, of which 12% mapped reads were outside of annotated genes and

1% could not be unambiguously assigned to one unique transcript. DEGs were identified from the remaining ~28.5 million reads per sample using the edgeR package (27) and the normalization procedure used in TMM (28). Biological outliers have a global effect on the differential analysis, reducing the robustness of the study. Therefore, to adjust for the influence of outliers on the DEGs, a model was generated using the function to estimate dispersion "estimateGLMRobustDisp", which consists of assigning a weight to each observation and the observations that strongly deviate from the model fit are assigned lower weights. This approach dampens the influence of outliers on the differential analysis while maintaining the robustness of the study (29). Finally, two separate generalized linear models of the DEGs were built for F_0 and F_3 to perform the analysis. Statistical significance was evaluated using the criteria of P value < 0.05. Results have been deposited in the Gene Expression Omnibus (GEO) database, www.ncbi.nlm.nih.gov/geo (BioProject ID: PRJNA481502).

Gene Network and Pathway analyses. DEGs were further analyzed for biological relevance using the IPA software (Ingenuity Systems). The corresponding human orthologs of the ZF genes from the DEG dataset were identified in the Ingenuity's Knowledge Base using HomoloGene as the reference database. A total of 11,176 (63%) probes were successfully mapped by IPA and for duplicated probes, the highest differential expression value was used for downstream analysis. Right-tailed Fisher's exact tests were used to compute P values to determine the probability that each enriched biological function and canonical pathway (i.e., well-characterized metabolic and cell signaling

pathways) assigned to that data set might be due to random chance. A P value < 0.05 was considered statistically significant.

The Gene Set Enrichment Analysis algorithm was also applied to the data set using Pathway Studio 10.0 (Ariadne) operating with the ResNet 11.0 database (Mammals). The corresponding human homologs of the ZF genes were identified using Ensembl (http://www.ensembl.org). If a human homolog could not be identified, the gene was not included in the pathway analysis. A total of 13,303 (74%) unigenes were successfully mapped in Pathway Studio and for duplicated probes, the option of "best P value, highest magnitude fold change" was used. A Kolmogorov–Smirnov test with 1,000 permutations was performed to determine whether specific gene sets were preferentially regulated compared to the background reference probability distribution. The gene set categories examined for enrichment included curated Ariadne cell processes, cell signaling and receptor signaling pathways. The enrichment P value for a gene-seed was set at $P < 0.05$.

Supplementary Figures

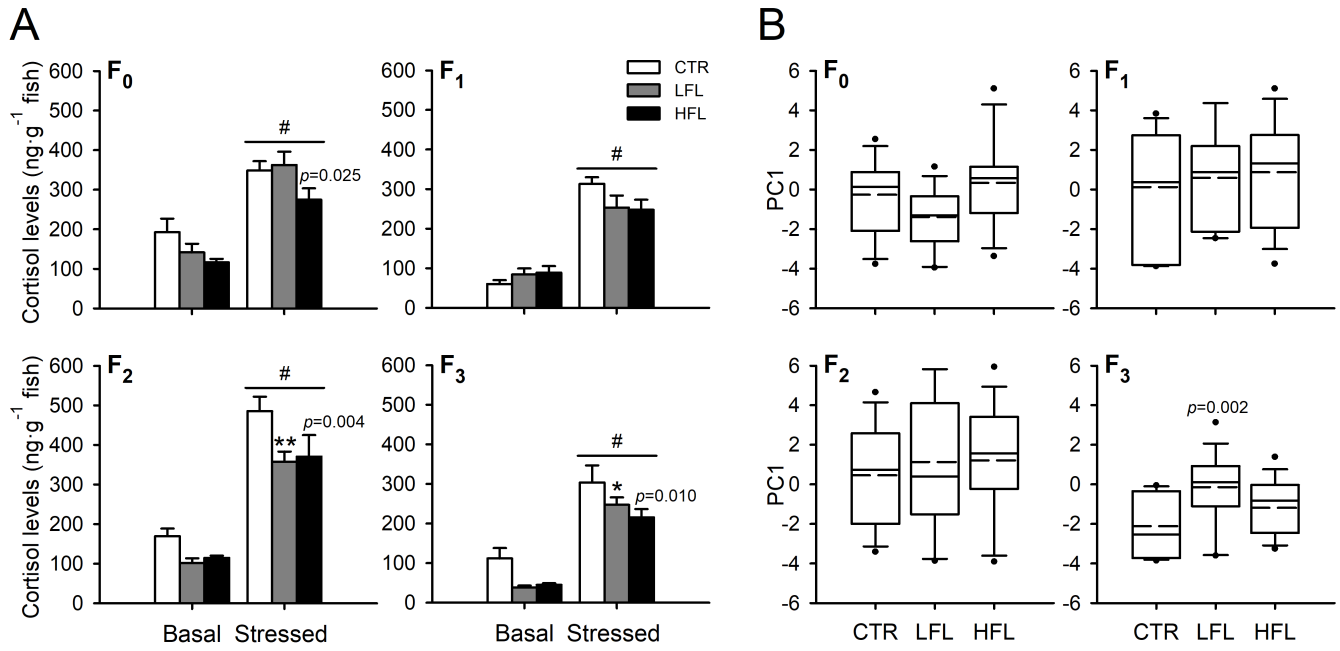

Fig. S1. Whole-body cortisol levels and behavioral analysis of adult female ZF from the CTR and FLX lineages. (*A*) Early-life FLX exposure to the F_0 reduced the basal and the net stress-induced cortisol levels of the F_0, F_2 and F_3 generations. $n = 6 – 10$ biological replicates per group. Data are presented as mean ± SEM and analyzed by two-way ANOVA (on ranks for F_2 and F_3). $^{\#}P < 0.001$ compared with the basal group. The asterisks (*) or *P* values shown above the bars represent significant difference in the FLX group compared with the CTR: $*P = 0.012$ and $**P < 0.001$. (*B*) FLX did not trigger any transgenerational alterations in female behavior following the novel-tank diving test (NTT). PCA was used to extract components comprised of linear combinations of 10 different behavioral metrics, which are related to the locomotor and exploratory behaviors of the fish. PC1 accounts for 59% of the variability of the dataset. $n = 13 – 17$ fish per group in each generation. Behavioral data are represented in box-and-whisker plots showing the upper and lower quartiles and range (box), median value (solid line), mean value (dashed line) and the 10^{th} and 90^{th} percentiles of the data (whiskers); all data outside the range of the whiskers are presented as individual data points. *P* values shown above the bars represent significant differences compared with the CTR analyzed by Student's *t*-test (or Mann-Whitney *U* test for HFL – F_1 and F_3).

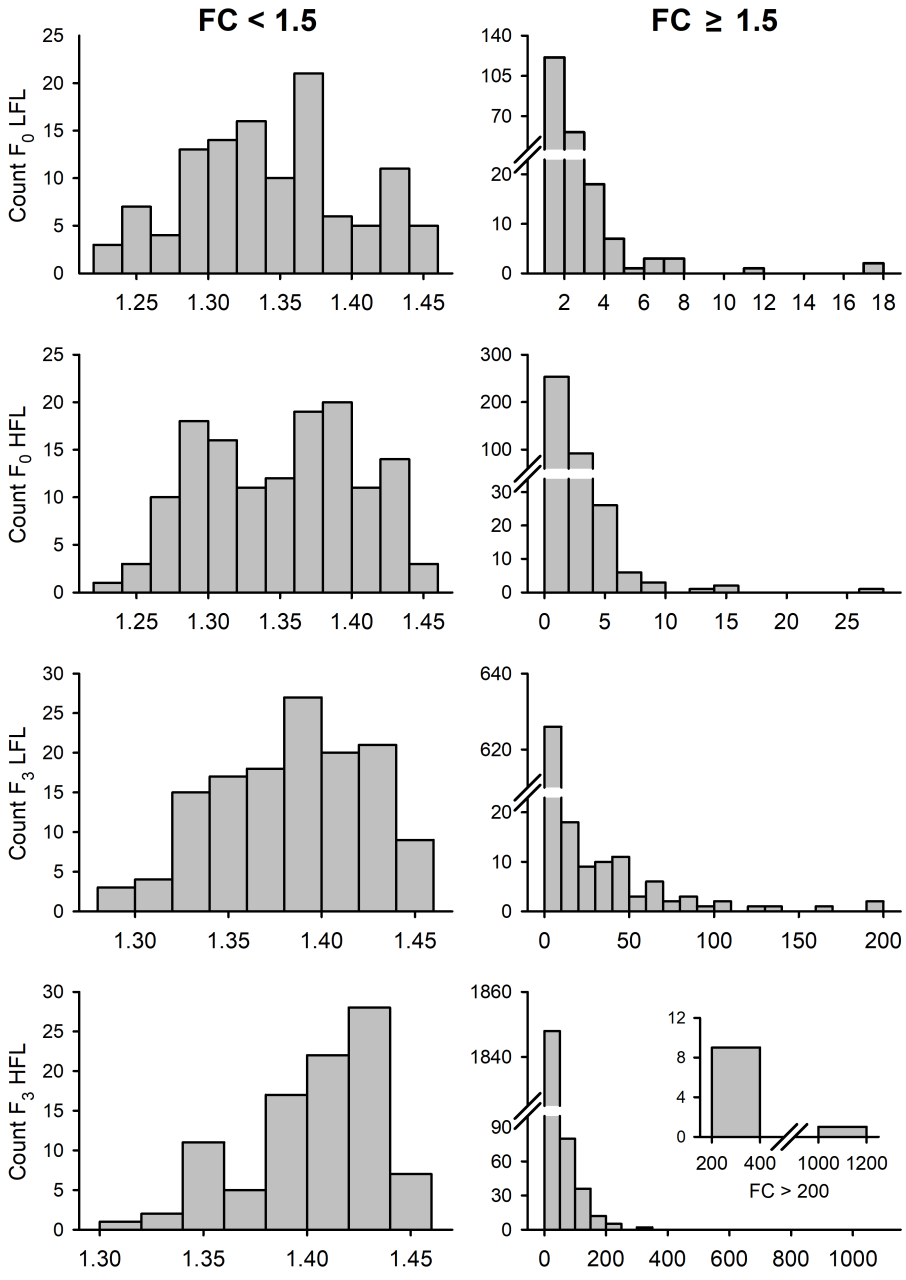

Fig. S2. Distribution of the DEGs according to their fold change (FC) across the FLX lineages (LFL, Low-FLX lineage; HFL, High-FLX lineage) from the F_0 and F_3 generations.

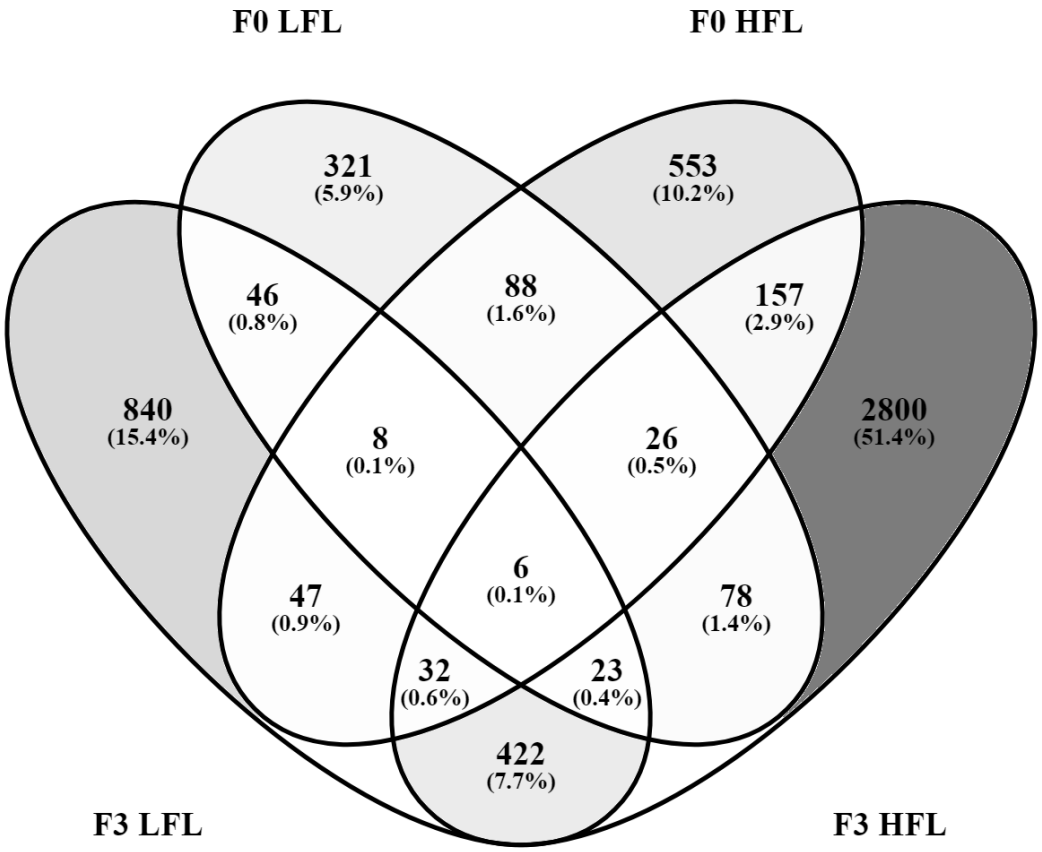

Fig. S3. Venn diagram illustrating the number of shared and uniquely differentially expressed genes ($P < 0.05$) in the male kidney among FLX lineages in the F_0 and F_3 generations. The two FLX lineages in F_3 shared the most differentially expressed genes and the HFL group in F_3 displayed the most uniquely differentially expressed genes (Venn diagram created using Oliveros (30)).

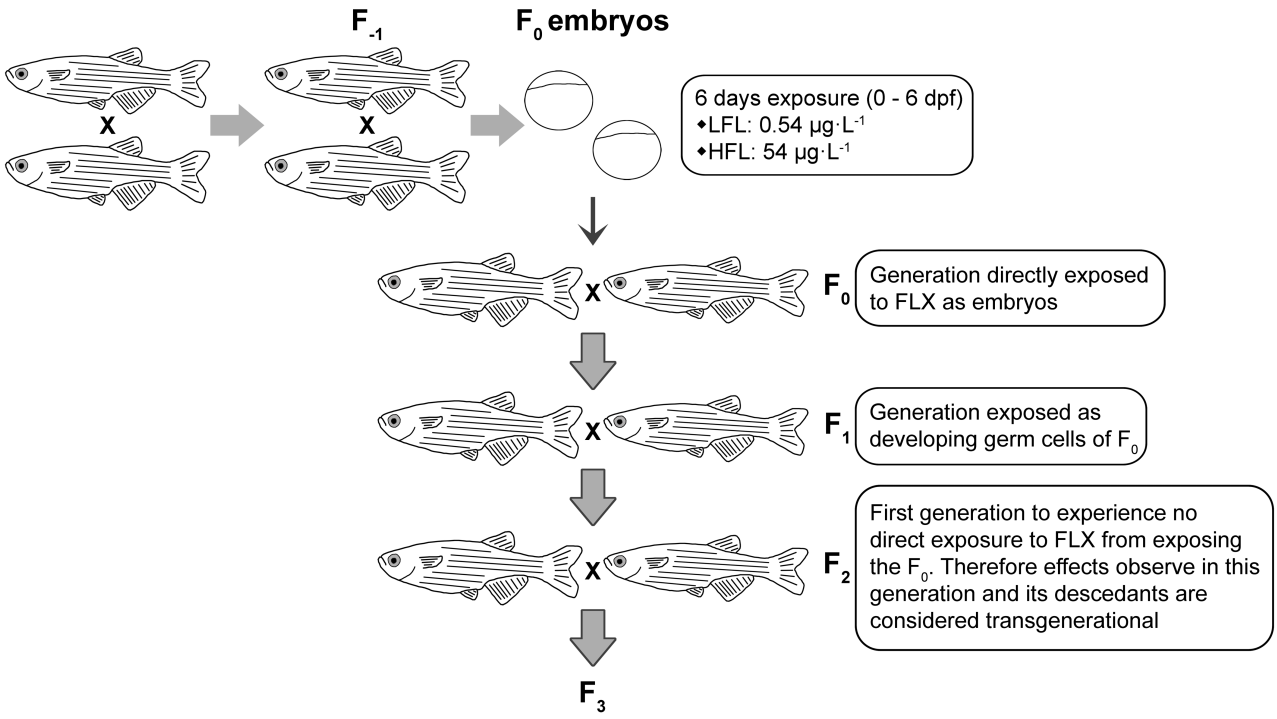

Fig. S4. Schematic representation of the ZF mating process to generate the CTR and the two FLX lineages. Adult ZF of the AB strain were mated to generate the F_{-1}, which was subsequently bred to produce the F_0. Exposure of F_0 as embryos to two FLX concentrations generated the FLX lineages for the F_1 to F_3 generations. The F_1 was exposed to FLX as developing germ cells when the F_0 embryos were being exposed. Therefore, only the effects observed in the F_2 and its descendants are considered transgenerational (31) since they have not experienced a direct exposure to FLX.

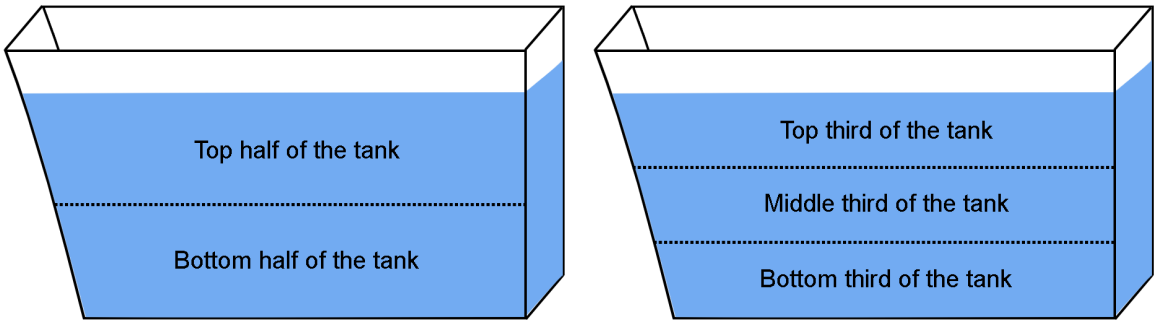

Fig. S5. The horizontal virtual divisions of the novel-tank diving test used to analyze the locomotor and exploratory behaviors of the fish. The left panel represents the divisions with two zones referred to as bottom half and top half of the tank. The right panel shows the three virtual divisions referred to as bottom third, middle third and top third of the tank.

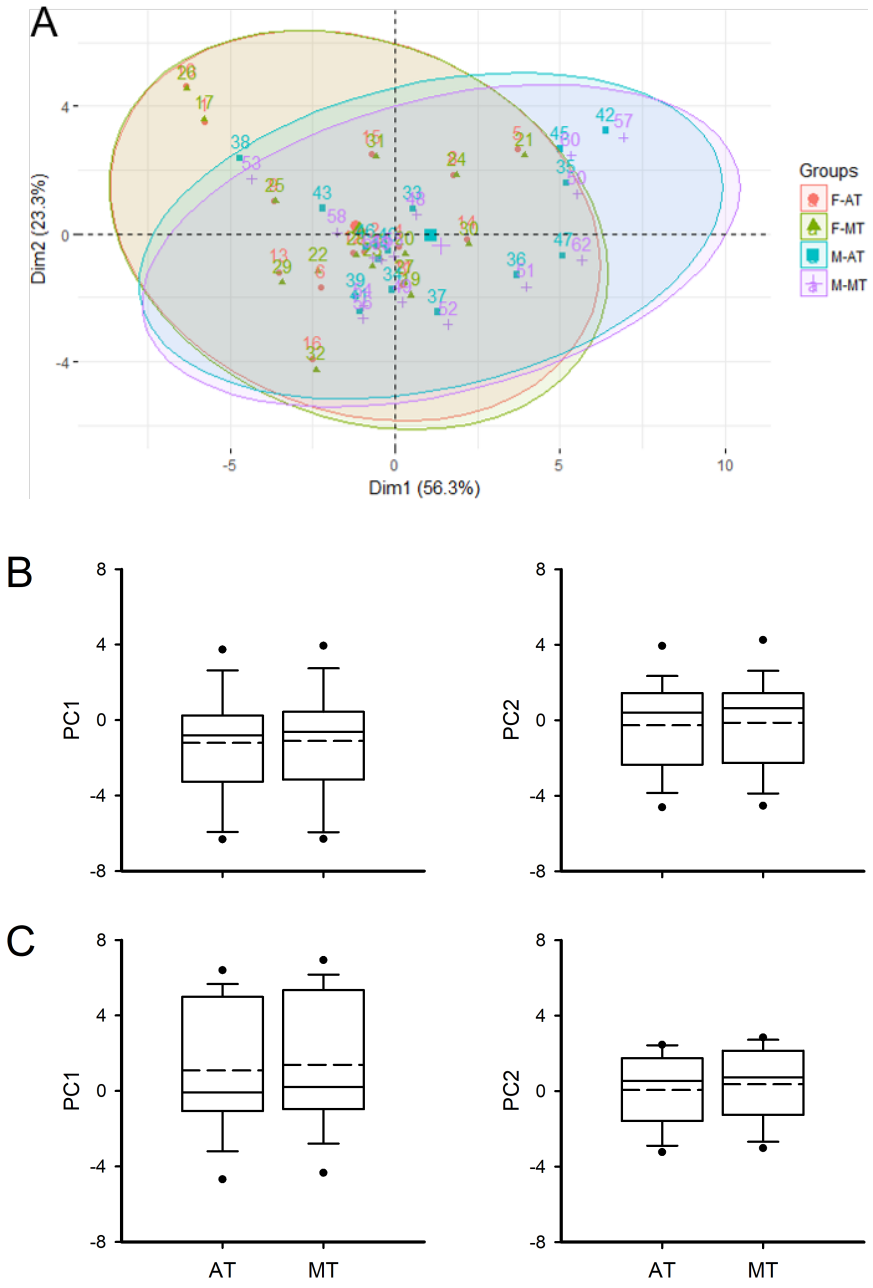

Fig. S6. Principal component analysis of the 18-behavioral metrics generated from tracking the behavioral response of adult ZF fish to the novel-tank diving test using the AT and MT algorithm. (*A*) Venn diagram illustrating PC1 (Dim1) and PC2 (Dim2) of the behavioral response of the females and males acquired from the two-different tracking software. (*B*) Box plot representation of the PC1 (*Left*) and PC2 (*Right*) of the females behavioral response. (*C*) Box plot representation of the PC1 (*Left*) and PC2 (*Right*) of the males behavioral response. n = 16 females and 15 males.

Supplementary Tables

Table S1. Behavioral metrics of the locomotor and exploratory behaviors following the novel-tank diving test computed using an automated tracking Python script.

Behavioral metrics	Units	Description
Latency middle third	s	Delay before entering the middle third of the tank
Latency top half	s	Delay before entering the top half of the tank
Latency top third	s	Delay before entering the top third of the tank
Transitions		Number of times the fish crossed into the top half of the tank
Time middle third	s	Total time spent in the middle third of the tank
Time top third	s	Total time spent in the top third of the tank
Distance middle third	cm	Total distance spent in the middle third of the tank
Distance top third	cm	Total distance spent in the top third of the tank
Total distance	cm	Total distance traveled around the tank
Max speed	$cm \cdot s^{-1}$	Maximum speed reached by the fish

Table S2. Loadings and contributions of the behavioral metrics to PC1

Behavioral metrics	Females		Males	
	Loadings	Contribution (%)	Loadings	Contribution (%)
Latency middle third	–0.295	8.7	–0.317	10.0
Latency top half	–0.358	12.8	–0.350	12.3
Latency top third	–0.358	12.8	–0.370	13.7
Transitions	0.374	14.0	0.373	13.9
Time middle third	0.362	13.1	0.385	14.8
Time top third	0.297	8.8	0.282	7.9
Distance middle third	0.375	14.0	0.393	15.5
Distance top third	0.332	11.1	0.308	9.5
Total distance	0.213	4.5	0.129	1.7
Max speed	–0.032	0.1	0.082	0.7

Table S3. *P* values of the top significant canonical pathways in the kidney of males from the F_0 and F_3 FLX lineages compared with controls

Canonical pathways	F_0		F_3	
	LFL	HFL	LFL	HFL
Antiproliferative Role of TOB in T Cell Signaling	**6.3×10^{-3}**	2.3×10^{-2}	NA	3.2×10^{-2}
Calcium Signaling	NS	2.8×10^{-2}	**1.3×10^{-3}**	3.1×10^{-3}
Caveolar-mediated Endocytosis Signaling	NS	**1.4×10^{-3}**	1.7×10^{-2}	1.5×10^{-2}
EIF2 Signaling	**5.6×10^{-3}**	NS	2.0×10^{-2}	1.0×10^{-4}
Epithelial Adherens Junction Signaling	NS	**7.4×10^{-4}**	4.9×10^{-2}	5.2×10^{-3}
ERK/MAPK Signaling	NS	2.1×10^{-2}	1.9×10^{-2}	**4.0×10^{-6}**
ILK Signaling	NS	**8.7×10^{-4}**	**4.7×10^{-4}**	**1.7×10^{-5}**
Integrin Signaling	NA	3.6×10^{-2}	1.9×10^{-2}	**4.7×10^{-7}**
Mitochondrial Dysfunction	**3.9×10^{-3}**	NS	**5.0×10^{-11}**	1.4×10^{-3}
Pancreatic Adenocarcinoma Signaling	3.2×10^{-2}	7.8×10^{-3}	NS	**1.6×10^{-5}**
Paxillin Signaling	NS	**1.5×10^{-3}**	1.0×10^{-2}	3.2×10^{-4}
RAR Activation	**5.2×10^{-4}**	5.8×10^{-3}	NS	1.9×10^{-3}
Remodeling of Epithelial Adherens Junctions	1.9×10^{-2}	**1.2×10^{-3}**	1.5×10^{-2}	1.7×10^{-3}
Sirtuin Signaling Pathway	**1.1×10^{-2}**	2.2×10^{-2}	**3.2×10^{-13}**	**4.8×10^{-7}**
TR/RXR Activation	NA	2.3×10^{-3}	**1.1×10^{-3}**	2.8×10^{-4}

NA, not available; pathway not detected.

NS, not significant.

P values in bold represent the top 5 significant canonical pathways in each of the treatments.

Table S4. Median fold change of enriched pathways following analysis using Pathway Studio ($P < 0.05$)

Enriched pathways	F_0		F_3	
	LFL	HFL	LFL	HFL
Biosynthesis of cholesterol	NA	0.48	0.49	0.19
Cholesterol catabolism	NA	2.73	NA	NA
Cholesterol export	2.14	NA	NA	0.42
Steroidogenesis	0.50	NA	2.05	0.38

NA, not available; pathway no detected.

Table S5. qRT-PCR analysis (fold change) of selected genes. For full gene names see Table S7

Gene symbol	F_0 LFL		F_0 HFL		F_3 LFL		F_3 HFL	
	RNA-seq	qRT-PCR	RNA-seq	qRT-PCR	RNA-seq	qRT-PCR	RNA-seq	qRT-PCR
ctgfa	–1.49*	–2.35*	1.05	–3.17*	–1.35	–1.45	–1.06	–2.03
cyp11a1	4.07*	1.13	–1.58	3.27	–1.82	–2.01*	1.32	–2.38
dhcr7	–1.27	1.36	–1.04	–1.25	–1.10	–1.84	–5.28*	–1.92
lcat	1.13	–1.08	1.37	–1.44	–1.58	–1.27	–215.03*	–1.93
lss	–1.05	–1.37	–2.25	–1.33	–2.65	–2.14	–13.29*	–4.75*
namptb	–1.12	–1.07	1.63*	–1.37	1.03	–1.55	–12.94*	–2.67*
pmvk	1.25	1.23	1.03	–1.27	–1.50	–1.14	–4.26*	–3.73*
rb1	–1.04	–1.46	–1.27	–2.25*	–1.10	1.24	–9.96*	–1.92*
star	1.16	8.42	1.03	26.54*	29.30*	218.58*	5.81	19.98
sts	–1.03	1.07	1.22	–1.29	–1.53	–1.15	–4.51*	–1.78

*P value < 0.05

Table S6. Average fold change ($P < 0.05$) of key transcripts associated with DNA and histones modifications in male ZF kidney from the F_0 and F_3 generations

Gene symbol	F_0		F_3	
	LFL	HFL	LFL	HFL
dnmt1	NS	–1.40	NS	NS
dnmt5	NS	NS	NS	–17.1
dnmt8	NS	NS	NS	–4.85
hdac4	NS	NS	NS	–10.8
hdac6	NS	NS	–1.61	NS

NS, not significant.

Table S7. List of primer sets (in alphabetical order) used to conduct qRT-PCR on male ZF kidney from the F_0 and F_3 generations

Gene symbol	Gene name	Primer sequence (5'→3')	GenBank ID
ctgfa	connective tissue growth factor a	F: GAAAGTGCCTGGGAAGTGCT R: TCCTCCTCTCTGTAAGCTGCTA	NM_001015041.2
cyp11a1	cytochrome P450 family 11 subfamily A polypeptide 1	F: CATTCCAGCAGGGACTTTAG R: CAGCGAGAGGGACAGTAT	NM_152953.2
dhcr7	7-dehydrocholesterol reductase	F: ATGACCTCTGGGTTTTGGGG R: TCCACAGGCCAAACAGTACG	NM_201330.1
lcat	lecithin-cholesterol acyltransferase	F: TGTGGGACGACACCAGAAAC R: AGTCCTACCCCATACAGGCA	NM_001324407.1
lss	lanosterol synthase (2,3-oxidosqualene-lanosterol cyclase)	F: AGAGTGCCTTACACAAGCCC R: GGGAAAGCCTCCCTTGTTCA	NM_001083567.1
namptb	nicotinamide phosphoribosyltransferase b	F: AGTGCTTCCGTCATACCTGC R: CACTCCAACCCTCATCGCTC	NM_212668.2
pmvk	phosphomevalonate kinase	F: GAGTCCGAGTGTGGTTTGGA R: TGACCGATGACAGAAGCTCG	NM_001083579.1
rb1	retinoblastoma 1	F: AGTCGCCCTACAATTCGGTG R: CAGGACGGGGTTTGCTTTTG	NM_001077780.1
star	steroidogenic acute regulatory protein	F: AGCCCTTGTTCAAGTCAGACG R: TGGCAAAGTGGAGGTGACAG	NM_131663.1
sts	steroid sulfatase (microsomal), isozyme S	F: GGCATGTTTCCACACTCA R: CTGTTGGGTCTTTGGATAGG	XM_005168397.4

Table S8. The percent differences of the complete list of behavioral metrics computed from the automated tracking (AT) Python script compared to the manual tracking conducted using Logger Pro

Behavioral metrics	Units	Description	% Difference
Latency middle third	s	Delay before entering the middle third of the tank	5.3
Latency top half	s	Delay before entering the top half of the tank	1.7
Latency top third	s	Delay before entering the top third of the tank	0.9
Transitions		Number of times the fish crossed into the top half of the tank	4.0
Time bottom third	s	Total time spent in the bottom third of the tank	0.3
Time middle third	s	Total time spent in the middle third of the tank	2.3
Time top third	s	Total time spent in the top third of the tank	4.9
Time bottom half	s	Total time spent in the bottom half of the tank	0.2
Time top half	s	Total time spent in the top half of the tank	2.4
Distance bottom third	cm	Total distance spent in the bottom third of the tank	3.4
Distance middle third	cm	Total distance spent in the middle third of the tank	4.6
Distance top third	cm	Total distance spent in the top third of the tank	6.7
Distance bottom half	cm	Total distance spent in the bottom half of the tank	3.4
Distance top half	cm	Total distance spent in the top half of the tank	6.0

Total distance	cm	Total distance traveled around the tank	3.5
Entry duration	s	Average time the fish spent in the top half of the tank	3.9
Mean speed	$cm \cdot s^{-1}$	Average speed of the fish	2.8
Max speed	$cm \cdot s^{-1}$	Maximum speed reached by the fish	8.0

Table S9. Loadings and contributions of the behavioral metrics to PC1 and PC2

Behavioral metrics	PC1		PC2	
	Loadings	Contribution (%)	Loadings	Contribution (%)
Latency middle third	–0.167	2.8	–0.303	9.2
Latency top half	–0.194	3.8	–0.233	5.4
Latency top third	–0.209	4.4	–0.115	1.3
Transitions	0.284	8.1	0.003	0.0
Time bottom third	–0.3	9.0	0.125	1.6
Time middle third	0.292	8.5	–0.072	0.5
Time top third	0.273	7.4	–0.206	4.2
Time bottom half	–0.291	8.5	0.172	3.0
Time top half	0.291	8.4	–0.172	3.0
Distance bottom third	0.054	0.3	0.453	20.5
Distance middle third	0.293	8.6	–0.017	0.0
Distance top third	0.264	7.0	–0.175	3.0
Distance bottom half	0.124	1.5	0.431	18.5
Distance top half	0.291	8.4	–0.137	1.9
Total distance	0.218	4.8	0.322	10.3
Entry duration	0.191	3.6	–0.206	4.3
Mean speed	0.22	4.8	0.319	10.2
Max speed	0.035	0.1	0.172	3.0

References

1. Hendrick V*, et al.* (2003) Placental passage of antidepressant medications. *Am J Psychiatry* 160(5):993-996.
2. Kim J*, et al.* (2006) Stereoselective disposition of fluoxetine and norfluoxetine during pregnancy and breast-feeding. *Br J Clin Pharmacol* 61(2):155-163.
3. Rampono J, Proud S, Hackett LP, Kristensen JH, & Ilett KF (2004) A pilot study of newer antidepressant concentrations in cord and maternal serum and possible effects in the neonate. *Int J Neuropsychopharmacol* 7(3):329-334.
4. Joana G & Zélia B (2016) Validation of two spectrophotometric methods for fluoxetine quantification. *Int J Pharm Pharm Sci* 8(3):72-78.
5. Rampono J*, et al.* (2009) Placental transfer of SSRI and SNRI antidepressants and effects on the neonate. *Pharmacopsychiatry* 42(3):95-100.
6. Preskorn S (1994) Targeted pharmacotherapy in depression management: comparative pharmacokinetics of fluoxetine, paroxetine and sertraline. *Int Clin Psychopharmacol* 9 Suppl 3:13-19.
7. Alboni S*, et al.* (2017) Fluoxetine effects on molecular, cellular and behavioral endophenotypes of depression are driven by the living environment. *Mol Psychiatry* 22(4):552-561.
8. Pan Y, Hong Y, Zhang QY, & Kong LD (2013) Impaired hypothalamic insulin signaling in CUMS rats: restored by icariin and fluoxetine through inhibiting CRF system. *Psychoneuroendocrinology* 38(1):122-134.
9. David DJ*, et al.* (2009) Neurogenesis-Dependent and -Independent Effects of Fluoxetine in an Animal Model of Anxiety/Depression. *Neuron* 62(4):479-493.
10. Mennigen JA*, et al.* (2010) Waterborne fluoxetine disrupts the reproductive axis in sexually mature male goldfish, *Carassius auratus*. *Aquat Toxicol* 100(4):354-364.
11. Mennigen JA, Stroud P, Zamora JM, Moon TW, & Trudeau VL (2011) Pharmaceuticals as neuroendocrine disruptors: lessons learned from fish on Prozac. *J Toxicol Environ Health B Crit Rev* 14(5-7):387-412.
12. Craig PM, Trudeau VL, & Moon TW (2014) Profiling hepatic microRNAs in zebrafish: fluoxetine exposure mimics a fasting response that targets AMP-activated protein kinase (AMPK). *PLoS One* 9(4):e95351.
13. Pyron M (2003) Female preferences and male-male interactions in zebrafish (*Danio rerio*). *Canadian Journal of Zoology* 81(1):122-125.
14. Spence R, Gerlach G, Lawrence C, & Smith C (2008) The behaviour and ecology of the zebrafish, *Danio rerio*. *Biol Rev Camb Philos Soc* 83(1):13-34.
15. Uusi-Heikkilä S, Böckenhoff L, Wolter C, & Arlinghaus R (2012) Differential allocation by female zebrafish (*Danio rerio*) to different-sized males--an example in a fish species lacking parental care. *PLoS One* 7(10):e48317.
16. Mueller T & Wullimann MF (2016) Chapter 2 - Atlas of cellular markers in zebrafish neurogenesis: Atlas. *Atlas of Early Zebrafish Brain Development (Second Edition)*, (Elsevier, San Diego), pp 27-157.
17. Matthews M, Trevarrow B, & Matthews J (2002) A virtual tour of the guide for zebrafish users. *Lab Anim (NY)* 31(3):34-40.

18. Castranova D*, et al.* (2011) The effect of stocking densities on reproductive performance in laboratory zebrafish (*Danio rerio*). *Zebrafish* 8(3):141-146.
19. Lawrence C (2007) The husbandry of zebrafish (*Danio rerio*): A review. *Aquaculture* 269(1):1-20.
20. Ribas L & Piferrer F (2014) The zebrafish (*Danio rerio*) as a model organism, with emphasis on applications for finfish aquaculture research. *Reviews in Aquaculture* 6(4):209-240.
21. Levin ED, Bencan Z, & Cerutti DT (2007) Anxiolytic effects of nicotine in zebrafish. *Physiol Behav* 90(1):54-58.
22. Wong K*, et al.* (2010) Analyzing habituation responses to novelty in zebrafish (*Danio rerio*). *Behav Brain Res* 208(2):450-457.
23. Rosemberg DB*, et al.* (2011) Differences in spatio-temporal behavior of zebrafish in the open tank paradigm after a short-period confinement into dark and bright environments. *PLoS One* 6(5):e19397.
24. Martin M (2011) Cutadapt removes adapter sequences from high-throughput sequencing reads. *EMBnet.journal* 17(1):10-12.
25. Dobin A*, et al.* (2013) STAR: ultrafast universal RNA-seq aligner. *Bioinformatics* 29(1):15-21.
26. Hartley SW & Mullikin JC (2015) QoRTs: a comprehensive toolset for quality control and data processing of RNA-Seq experiments. *BMC Bioinformatics* 16:224.
27. Robinson MD, McCarthy DJ, & Smyth GK (2010) edgeR: a Bioconductor package for differential expression analysis of digital gene expression data. *Bioinformatics* 26(1):139-140.
28. Robinson MD & Oshlack A (2010) A scaling normalization method for differential expression analysis of RNA-seq data. *Genome Biol* 11(3):R25.
29. Zhou X, Lindsay H, & Robinson MD (2014) Robustly detecting differential expression in RNA sequencing data using observation weights. *Nucleic Acids Res* 42(11):e91.
30. Oliveros JC (2007-2015) Venny. An interactive tool for comparing lists with Venn's diagrams.
31. Aluru N (2017) Epigenetic effects of environmental chemicals: insights from zebrafish. *Curr Opin Toxicol* 6:26-33.